A METHOD FOR EVALUATING THE FATIGUE CRACK GROWTH IN SPIRAL NOTCH TORSION FRACTURE TOUGHNESS TEST

J.-A. Wang[1], T. Tan[2]

[1]*Oak Ridge National Laboratory, Materials Science & Technology Division, Oak Ridge, Tennessee 37831, USA*
[1]*Corresponding author: e-mail address: wangja@ornl.gov*
[2]*University of Vermont, Department of Civil Engineering, Burlington, Vermont 05405, USA*

Abstract: The Spiral Notch Torsion Test (SNTT) has been a recent breakthrough in measuring fracture toughness for different materials, including metals, ceramics, concrete and polymers composites. Due to its high geometry constraint and unique loading condition, SNTT can be used to measure the fracture toughness with smaller specimens without concern of size effects. The application of SNTT to brittle materials has been proved to be successful. The micro-cracks induced by original notches in brittle materials could ensure crack growth in SNTT samples. Therefore, no fatigue pre-cracks are needed. The application of SNTT to the ductile material to generate valid toughness data will require a test sample with sufficient crack length. Fatigue pre-crack growth techniques are employed to introduce sharp crack front into the sample. Previously, only rough calculations were applied to estimate the compliance evolution in the SNTT crack growth process; while accurate quantitative descriptions have never been attempted. This generates an urgent need to understand the crack evolution during the SNTT fracture testing process of ductile materials. The newly developed governing equations for SNTT crack growth estimate are discussed in the paper.

Keywords: spiral notch torsion test, fracture toughness, fatigue pre-crack

1. Introduction

A basic postulate of fracture mechanics is the existence of a flaw that raises the local stress level in the material and produces fracture when the stress level reaches a critical value. The measure of fracture toughness is represented in terms of stress-intensity factor. The Mode I (tensile opening mode) stress-intensity factor at the onset of rapid crack propagation under plane-strain conditions is defined as fracture toughness, K_{IC}, a controlling reference parameter used in design to avoid catastrophic brittle fracture. ASTM standard test methods, Standard Test Method for Plane-Strain Fracture Toughness of Metallic Materials (E399), are widely used to determine fracture toughness of metallic materials, using compact tension and compact disk tension specimens having thickness and volume sufficient to ensure the plane-strain condition at the crack front. Therefore, the accuracy and reliability of test results may be questionable if the specimen becomes excessively smaller than the minimum specimen size recommended by ASTM standard. If it is not possible to make a specimen from the available material that meets the criteria specified in E399, then it is not possible to make a valid K_{IC} measurement according to E399. Meeting the requirements is difficult and impractical because engineering systems materials to be investigated may be geometrically unsuitable and/or have insufficient volume for making the standard specimen. Therefore, use of small specimens for K_{IC} measurement is essential for application to engineering structure safety evaluation under target service environment. Clearly, there is a need for a new method to obtain valid data using small samples. Despite the international efforts on the development of small specimen testing techniques, no methods currently exist for direct measurement of K_{IC} for small specimens without concern for size effect. Unlike the conventional test methods, the spiral notch torsion test (SNTT) method is capable of testing small rod specimens that bear no resemblance to conventional compact tension specimens nor using conventional mode of loading [1-6]. Therefore, the SNTT method is unique and innovative in both specimen design and loading concept.

Fig. 1 SNTT configuration.

The SNTT system, shown in Fig. 1, was developed to measure the intrinsic fracture toughness (K_{IC}) of structural materials, overcomes

many of the limitations inherent in traditional techniques, and introduces new possibilities for standardizing fracture toughness testing using small or miniature specimens. The system is uniquely suited to test a wide variety of materials, such as metals and alloys, ceramics, composites, thin-film coating, polymers, and concrete [7-12], and for pressure vessel steel in-situ hydrogen embrittlement study [13-14]. The SNTT system operates by applying pure torsion to cylindrical specimens machined with a notch line that spirals around the specimen at a 45° pitch. The fractured miniature SNTT specimen is shown in Fig. 2.

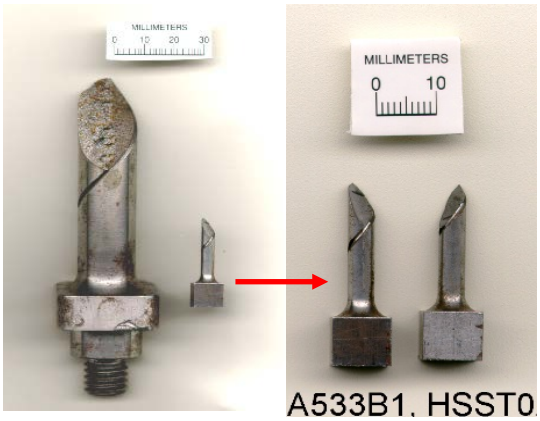

Fig. 2 Fractured SNTT specimens: (a) A302B, and (b) A533B miniature sample.

SNTT methodology is shown in Fig. 3a, which shows that the principle tensile stress (opening mode) is perpendicular to the 45° spiral groove line, and crack propagation is toward and perpendicular to the specimen central axis. Fig. 3b illustrated the SNTT is the direct transformation of CT specimen. The CT specimen, as shown in the upper area of Fig. 3b, has been widely used in existing fracture toughness test methods because the general consensus indicates it is the next-best basic configuration that nearly conforms to the strict requirements of the classical theory of fracture mechanics. Despite the simplification, the theoretical conditions (i.e., the conditions required to achieve uniformly distributed applied stress over the thickness and plane-strain condition) can never materialize as long as the free surfaces exist at both ends. The end effects will be further amplified when the thickness decreases to a thin plate, as shown in Fig. 3b. Another dilemma is that an increase in specimen thickness will automatically accompany an increase in specimen length and width in order to maintain specimen rigidity under load. Miniaturization is an important goal of SNTT method. This is made possible because the K_{IC} values determined by the SNTT method are virtually independent of specimen size. A cursory review of the stress and strain fields in a CT specimen indicates that the key information needed for determining the K_{IC} values is manifested within a small region near the crack tip; therefore, the rod specimen can be miniaturized substantially without the loss of general validity (Fig. 3b). The purpose of the vast volume of the material outside the critical zone in conventional samples is to poise the ideal far field of stress and to provide a means to accommodate loading devices. This redundancy is eliminated to the optimum condition in the round rod specimen; therefore, the specimen miniaturization is achievable.

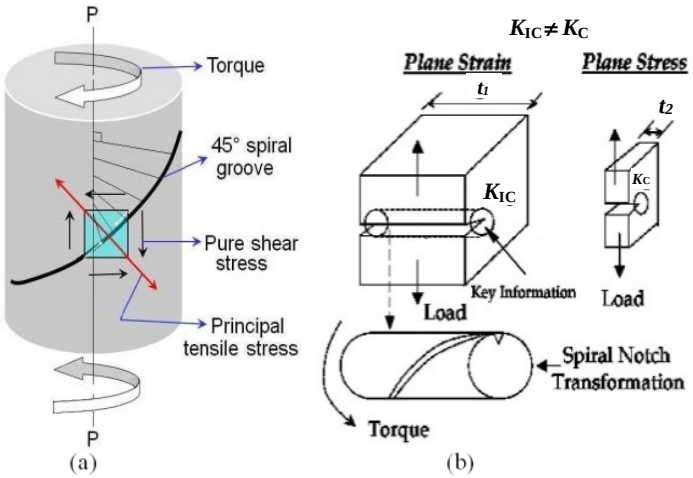

Fig. 3 (a) Schematic of SNTT theory, (b) CT and SNTT specimens' comparison and specimen size effect.

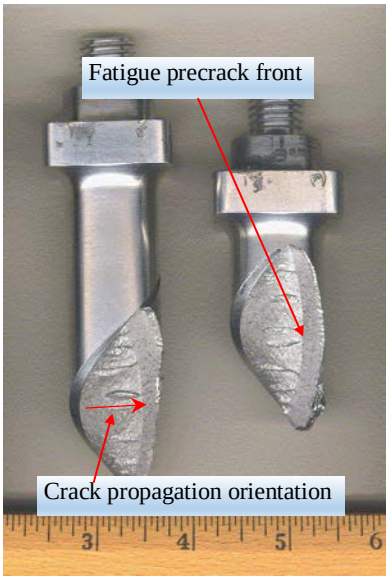

Fig. 4. Fatigue precrack SNTT sample of 7475 aluminum.

Furthermore, due to the plane strain and axisymmetric constraint and the uniformity in the stress and strain fields of SNTT configuration, the crack front must propagate perpendicularly toward the specimen axis along the conoids. Post-mortem examination verified the crack propagation behavior (see Fig. 4),

which reveals very uniform crack front and crack propagation is perpendicular to the specimen center axis.

To obtain valid results for brittle materials under conventional test conditions, a deep notch and fatigue precracking is required to develop a sharp crack front. The SNTT system with shallow notch does not require a fatigue precrack to obtain valid results for brittle samples. Such as for the SNTT test on mullite ceramic material sample, a shallow spiral V-groove with a depth of 0.5-mm on the uniform gage section of 17-mm diameter rod sample was sufficient for determining a valid K_{IC} values; the fractured mullite SNTT sample is shown in Fig. 5, which shows a tensile fracture surface profile.

Fig. 5 SNTT mullite sample.

In typical fracture toughness tests, the direction of crack propagation is unpredictable and often deflects in zigzags or in a parabolic "thumbnail" profile, both of which yield inconsistent data. When a sample is tested in the SNTT system, the spiral notch provides a consistent location for cracking to start, and the pure torsion load ensures that the crack will advance perpendicularly toward the central axis of the test specimen. This consistent cracking behavior eliminates much of the uncertainty inherent in conventional techniques. Cracking is inherently consistent in spiral notch specimens; thus, the crack characteristics are controllable, and K_{IC} values can be determined reliably.

2. The evolution of SNTT compliance and fracture resistance for ductile materials

Development of SNTT fatigue crack growth protocols in addition to single notch front geometry is essential for SNTT method in applying to ductile materials. The crack growth behavior of SNTT testing protocols has been effectively established using an integrated experimental, numerical and analytical approach, as illustrated in this section. The results indicate that the proposed protocol not only provides a significant advance in understanding the compliance evolution of the SNTT specimen, but also can be readily utilized to assist future developments in engineering structural materials performance reliability investigation.

Systematic studies show that the SNTT-type specimen can effectively simulate the behavior of a thick compact-tension specimen with thickness equal to the spiral groove length of the SNTT sample. Finite element simulations were performed to obtain the energy release rates at different crack lengths (depth) with the corresponding torques and rotation angles. By summarizing these numerical results, the evolution of the SNTT compliance and the energy release rates were studied with respect to different crack lengths. Two non-dimensional indices, the characteristic compliance and the characteristic energy release rates of SNTT, were proposed to quantify the crack growth process of SNTT. Collapse trends were observed between SNTT samples with different dimensions, as well as between samples made from both steel and aluminum. Analytical models in both broken and unbroken ligament forms were proposed to quantify the crack penetration depth based on these non-dimensional indices. The sensitivity in the broken-ligament form facilitates the experiment measurements, which could be easily adapted by industrial communities.

Fig. 6(a) shows the systematic evolution of the crack growth in the SNTT sample with FEA simulations; where the diameter of the cylinder is D. and a is the crack length. The ratio of crack length over diameter increases from 0.10 to 0.45. The length of each model is the same during the crack growth process. Fig. 6(b) shows the FEA deformation results for a/D=0.1 under end rotation of 0.002 radian. Based on FEA simulations and experimental verification input, the evolution of the compliance function and energy release rate were developed as shown in Figs. 7-8.

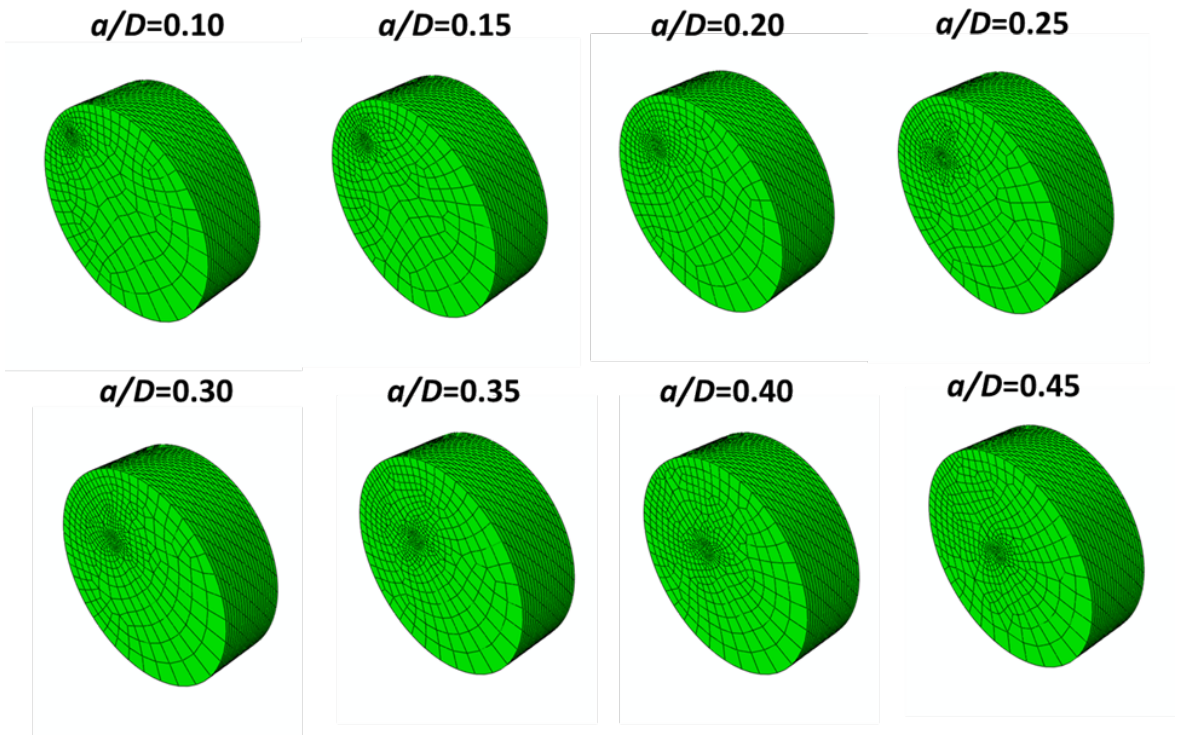

(a)

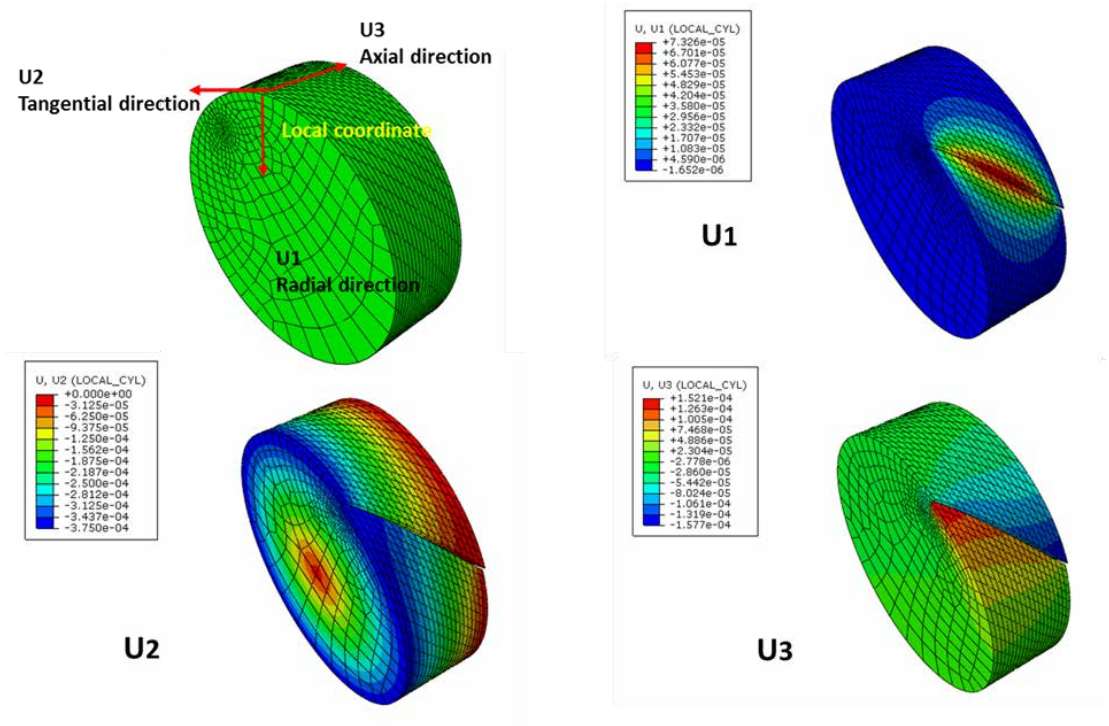

(b)

Fig.6 (a) The evolution of crack growth in the SNTT sample with FEA simulation models. (b) Single crack depth example FEA displacement results, for *a/D*=0.10, *D*=0.375-inch, Steel, under end rotation theta=0.002.

Detailed studies show that the evolutions of compliance and fracture resistance of the SNTT sample during the crack growth process can be unified together irrespective of specimen sizes and material types. The evolutions of compliance and fracture resistance in SNTT process were formulated with simple compliance governing equations as function of the ratios of crack lengths vs. the cylindrical diameter.

The finite element simulations were established with different crack lengths for selected SNTT specimens verified by physical measurements. Where steel and aluminum SNTT specimens were selected with two diameters of 1.0 inch and 0.375 inch for analysis. The objective was to obtain the evolutions of both compliance and the fracture resistance during the crack growth process for different types of SNTT samples.

Figs. 7-8 show the evolution of crack growth in an SNTT sample with *a/D* ratio increases from 0.10 to 0.45. Fig. 7a shows the compliance evolution of the SNTT sample with respect to different ratios of crack length over diameter. To obtain a more sensitive response of the compliance evolution, a factor was applied to account for the effect of unbroken ligament of the SNTT samples, which is graphed in Fig. 7b. It shows that the compliance evolution curves are the same for specimens with different materials or sizes. γ is the unit end rotation angle; T is the applied torque; μ is the shear modulus; and R is the cylinder radius.

Fig. 8a shows the fracture resistance evolution of the SNTT sample with respect to crack length over diameter ratios. In order to obtain a more sensitive response of the compliance evolution, a factor also was applied to account for the effect of unbroken ligament of the SNTT samples, which is shown in Fig. 8b. It was noted that fracture resistance curves are the same for specimens with different materials or sizes. G is the energy release rate; T is the applied torque; θ is the associated rotation angle; A is the cross-section area of the cylinder.

Unscaled SNTT Crack Growth Compliance Equation

$$\frac{\gamma}{T}\mu R^4 = -0.6541\left(\frac{a}{D}\right)^4 + 0.5189\left(\frac{a}{D}\right)^3 + 1.7171\left(\frac{a}{D}\right)^2 + 0.2045\left(\frac{a}{D}\right) + 0.6254$$

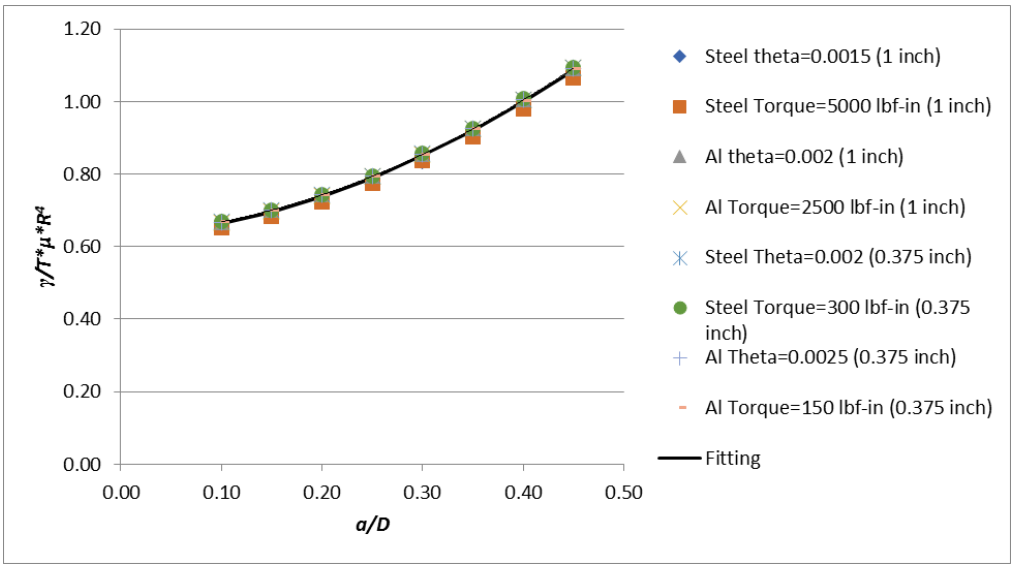

(a)

Scaled SNTT Crack Growth Compliance Equation

$$\frac{\gamma}{T}\mu R^4\left(1-\frac{a}{D}\right)^4 = 3.3445\left(\frac{a}{D}\right)^4 - 5.2514\left(\frac{a}{D}\right)^3 + 4.0568\left(\frac{a}{D}\right)^2 - 2.2298\left(\frac{a}{D}\right) + 0.6226$$

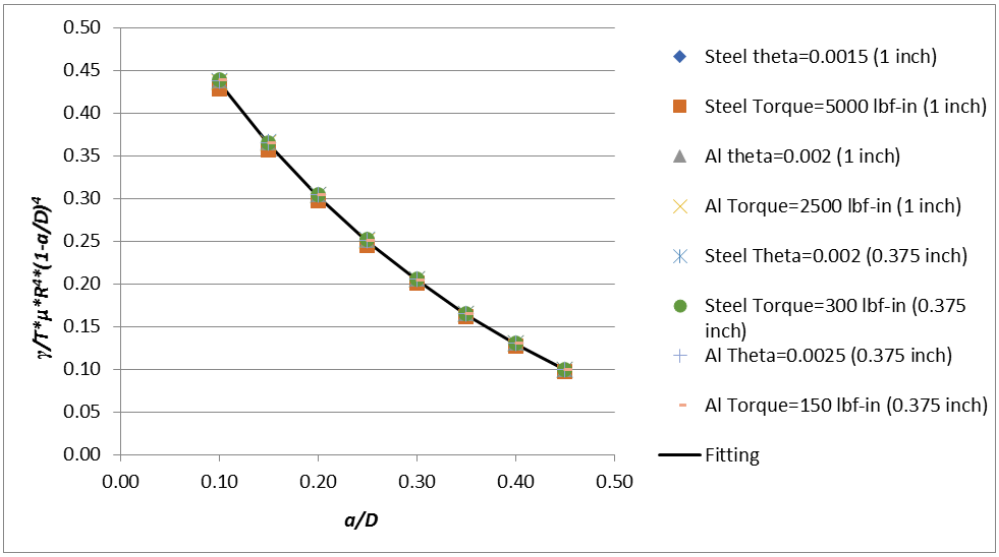

(b)

Fig. 7 (a) The unscaled compliance evolution with the crack growth; (b) The scaled compliance evolution along the crack growth with unbroken ligament factor.

Unscaled SNTT Energy Release Rate Evolution Equation

$$\frac{G*A}{T*\theta} = -95.543\left(\frac{a}{D}\right)^4 + 107.14\left(\frac{a}{D}\right)^3 - 52.72\left(\frac{a}{D}\right)^2 + 16.028\left(\frac{a}{D}\right) - 0.2489$$

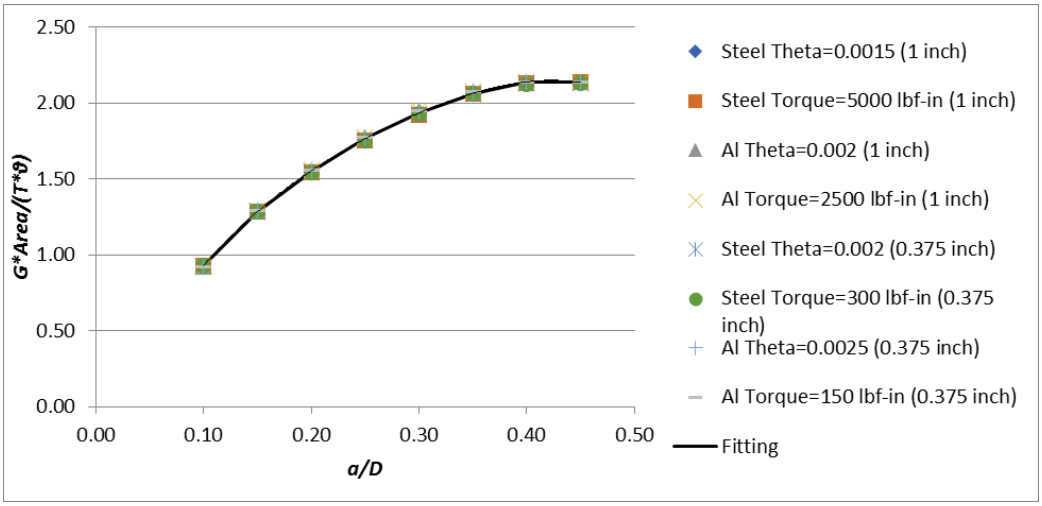

(a)

Scaled SNTT Energy Release Rate Evolution Equation

$$\frac{G*A}{T*\theta*\left(1-\frac{a}{D}\right)^2} = -154.56\left(\frac{a}{D}\right)^4 + 188.95\left(\frac{a}{D}\right)^3 - 62.398\left(\frac{a}{D}\right)^2 + 20.626\left(\frac{a}{D}\right) - 0.4716$$

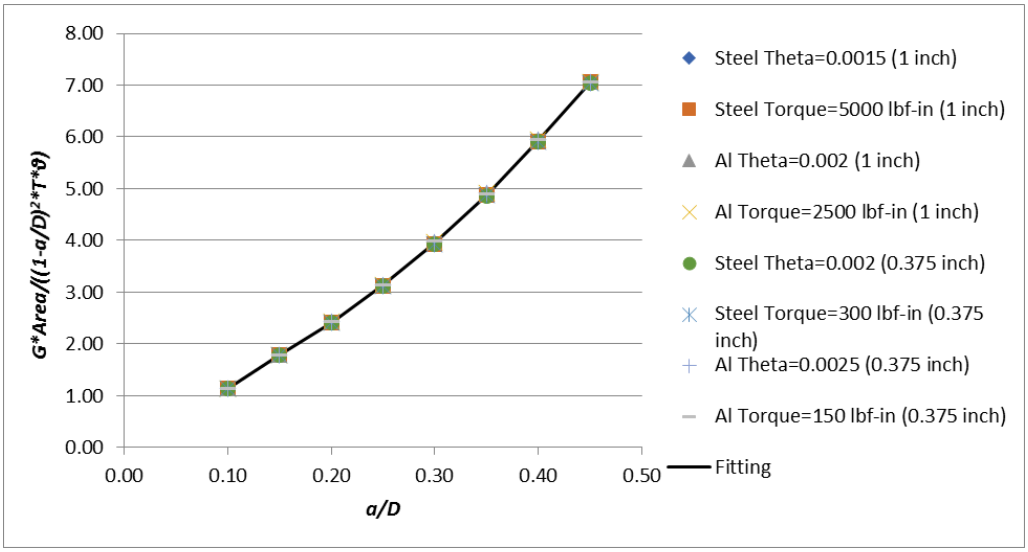

(b)

Fig. 8(a) The unscaled energy release rate evolution with the crack growth; (b) The scaled energy release rate evolution along the crack growth with unbroken ligament factor.

2.1 *Experimental verification on the developed SNTT fatigue protocol*

Experiment verification measurements were performed at different crack lengths during the cycle fatigue process. Specimens were cut in cross sections, and crack penetration depths were measured and compared with predictions from the developed SNTT compliance function. For the base material X52 pipe steel, a generally good agreement was observed between predictions and the experimental measurement. For the welded X52 materials, good agreements were also observed for most specimens. For some weld samples, crack deviation was observed during the cycle fatigue process. The reason for this deviation is mainly related to the flaws/impurities distribution of the welded material encountered in the fatigue precrack propagation path, based on postmortem examination. In order to validate the analytical models, further analysis was carried out on the rotary variable differential transformer (RVDT) measurement and finite element model predictions. The net section of the SNTT specimen was modeled with the measured crack depth. By using the torque data from the RVDT measurement, good agreement was observed between the predictions and the measurement.

X52 weld SNTT samples were fabricated from a segment of friction stir welded X52 steel pipe. The thickness of the pipe is 0.5 inch and the diameter of SNTT samples was designed as 0.375 inch accordingly. The SNTT specimen axis was parallel to the pipe cylinder axis. One complete loop of spiral groove was machined on the X52 SNTT sample. The fractured X52 baseline SNTT sample is shown in Fig. 9a, the detailed fatigue precrack area is shown in Fig. 9b, and the cross-section of fractured X52 weld SNTT sample is illustrated in Fig.9c.

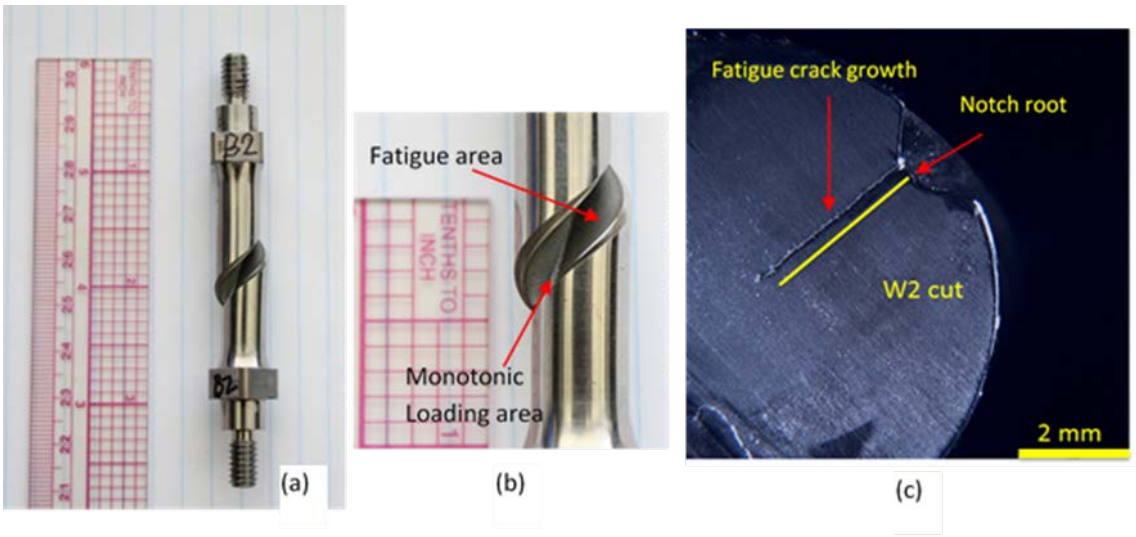

Fig. 9 The failed B2 specimen of X52 baseline sample, (a) entire view; (b) enlarged view of the middle section of tested SNTT sample, (c) the fatigue pre-crack growth profile of X52 weld SNTT sample W2, where the crack growth orientation is toward the central axis of the SNTT sample.

3. Conclusions

Systematic studies reveal that an SNTT-type specimen (a rod-type specimen having a helical groove with a 45-degree pitch) can effectively simulate the behavior of a thick compact-tension specimen equal to the total length of the groove line. Detailed studies show that the evolutions of compliance and fracture resistance of the SNTT sample during the crack growth process can be unified together irrespective of specimen sizes and material types. In addition to the special features of small volume specimen and ease of testing with the SNTT method, the independence of size effect is in rigorous analytical results for this testing method. The evolution of compliance and fracture resistance in the SNTT process has also been presented with simple governing equations using the ratios of crack lengths over the cylindrical diameter.

Based on the measured torques and rotation angles, the penetrated crack depth can be obtained through developed compliance governing equation. Once crack depths are known, the energy release rates, i.e., the crack driving force, can be obtained from the fracture resistance governing equation for the SNTT fatigue pre-crack experiments. Therefore, it is possible to control the crack penetration depth of SNTT experiment via monitoring the applied torques and rotation angles, which can be easily implemented by industrial communities.

Acknowledgement

This project is sponsored by U.S. Department of Energy (DOE) and Oak Ridge National Laboratory Seed Money Program, and U.S. Department of Transportation Pipeline and Hazardous Materials Safety Administration (PHMSA) Program. Oak Ridge National Laboratory is managed by UT-Battelle, LLC for the U.S. Department of Energy under Contract DE-AC05-00OR22725.

References

[1] Wang, J.-A., et.al., 2000. Using torsional bar testing to determine fracture toughness, Fatigue & Fracture of Engineering Materials & Structures Journal, **23**, 917-927.

[2] Wang, J.-A., Liu, K., "A New Approach to Evaluate Fracture Toughness of Structural Materials," Journal of Pressure Vessel Technology, Vol. 126, pp 534-540, 2004.

[3] Wang, J.-A., et.al., 2006. A new approach for evaluating thin film interface fracture toughness, Journal of Materials Science and Engineering A, **426** 332-345.

[4] Wang, J.-A., Kidane, A., “A new Approach to Determine the Quasi-static and Dynamic Fracture Toughness of Materials,” SEM XII International Congress & Exposition on Experimental & Applied Mechanics, Orange County/Costa Mesa, June 11-14, 2012.

[5] Bayles, R., Singh, R., Knight, S., Wang, J.-A., “Evaluating Stress-Corrosion Cracking Susceptibility Using a Torsion Test,” 2005 ASME Pressure Vessel Piping Conference, July 17-21, 2005, Denver, Colorado.

[6] Wang, J.-A., “Oak Ridge National Laboratory Spiral Notch Torsion Test System,” Journal of Practical Failure Analysis, Vol. 3(4) August 2003.

[7] Wang, J.-A., Liu, K., 2008. An innovative technique for evaluating fracture toughness of graphite materials, Journal of Nuclear Materials, **381**, 77-184.

[8] Wang, J.-A., Liu, K., Naus, D., 2010. A new test method for determining the fracture toughness of concrete materials, Journal of Cement and Concrete Research, **40**, 497-499.

[9] Tan, T., Ren, F., Wang, J.-A., et.al., 2013. Investigating fracture behavior of polymer and polymeric composite materials using spiral notch torsion test, Journal of Engineering Fracture Mechanics, **10**, 109-128.

[10] Ren, F., Wang, J.-A., Bertelsen, W., “Fractographic study of epoxy materials fractured under mode I loading and mixed mode I/III loading”, Materials Science and Engineering A, Vol. 532, p. 449-455, 2012.

[11] Bayles, R., King, S., Wang, J.-A., “Application of Disc Compact Tension Formulas to Compliance and K-Calibration of Spiral Notch Torsion Test Specimens,” 6th International Aircraft Corrosion Workshop, August 24-27, 2004 at the Holiday Inn Select, Solomons, Maryland.

[12] Wang, J.-A., Wright, I., et.al., “Interface Fracture Toughness Evaluation for MA956 Oxide Film,” Proceeding of 2005 ASM International Surface Engineering Congress, pp 80-89, August 1-3, 2005, St. Paul, Minnesota.

[13] Zhang, W., Feng, Z., Wang, J.-A., "Measurement of Fracture Toughness of Materials with Non-uniform Microstructure by Spiral Notch Torsion Test," 2010 ASME PVP Conference, July 18-22, 2010, Washington.

[14] Wang, J.-A., Ren, F., Tan, T., Liu, K., “The development of in situ fracture toughness evaluation techniques in hydrogen environment,” International Journal of Hydrogen Energy, 40 (2015) p.p. 2013-2024, January 2015.